

MATHEMATICAL MODEL FOR PREDICTING THE MAXIMUM WATER DEMAND OF CROPS

BOUZO, C. A.¹ & NORERO SCH, A. L.²

ABSTRACT

Diverse methods with different levels of complexity exist for the calculation of crop evapotranspiration. The understanding and quantification of evapotranspiration has advanced with the emergence of mathematical models to estimate the water demand of crops. The objective of this work is developing a mathematical model for the maximum water demand of crops, depending on phytometric and meteorological characteristics. The model is based on two main concepts: the maximum evapotranspiration and the energetic balance in the crops. The model was coded as macros of Visual Basic to be used in Microsoft® Excel. The model discriminates functional from structural variability of the micro-meteorology in the canopy. The model results for crops of cotton (*Gossypium hirsutum* L.), sunflower (*Helianthus annuus* L.), corn (*Zea mays* L.) and potato (*Solanum tuberosum* L.), showed a good agreement with data from the Penman-Monteith method.

Key words: Maximum evapotranspiration; Energetic balance; Radiation balance; Simulation.

RESUMEN

Modelo matemático para predecir la demanda máxima de agua de los cultivos.

En el cálculo de la evapotranspiración de los cultivos existen métodos con diferentes grados de complejidad. La aparición de modelos matemáticos para estimar la demanda de agua de los cultivos significó un avance en la comprensión y cuantificación de la evapotranspiración. El objetivo de este trabajo fue desarrollar un modelo matemático para estimar la demanda máxima de agua en cultivos agrícolas dadas algunas características fitométricas y meteorológicas. El modelo se desarrolló considerando dos conceptos principales: el de evapotranspiración máxima y balance energético de los cultivos. El mismo fue codificado con macros de Visual Basic para su uso con Microsoft® Excel. Finalmente, los resultados obtenidos permitieron discriminar en lo funcional y estructural la variabilidad de la micrometeorología en el dosel de varios cultivos. Se compararon

1.- Facultad de Ciencias Agrarias (UNL). Kreder 2805. (3080) Esperanza, provincia de Santa Fe.
E-mail address: cbouzo@arnet.com.ar

2.- Facultad de Agronomía e Ingeniería Forestal, Pontificia Universidad Católica de Chile. Casilla 306.
Santiago 22, Chile.

Manuscrito recibido el 12 de febrero de 2015 y aceptado para su publicación el 20 de mayo de 2015.

algunos resultados del modelo para cultivos de algodón (*Gossypium hirsutum* L.), girasol (*Helianthus annuus* L.), maíz (*Zea mays* L.) y papa (*Solanum tuberosum* L.) con datos provenientes del método de Penman-Monteith, habiéndose obtenidos aceptables aproximaciones.

Palabras clave: Evapotranspiración máxima; Balance energético; Balance de radiación; Simulación.

INTRODUCTION

The water demand in crops is directly related to the evapotranspiration (ET). Two separated processes contribute to ET: water is lost thorough the surface by evaporation and also by transpiration of the crop (Allen *et al.*, 1998). Some of the variables to quantify this phenomenon are: (i) potential evapotranspiration (ETP), that is, the loss of water from a surface with vegetation with no hydric deficit (Lu *et al.*, 2005); (ii) reference evapotranspiration (ET_o), that is, evapotranspiration occurring in an extensive surface of 8 to 15 cm tall green grass, in active growth, and totally covering the soil (Doorenbos & Kassam, 1980).

Methods to determine evapotranspiration are classified in direct, also called measurement methods, and indirect (Sánchez Martínez, 2001). Direct methods are numerous, among them, use of lysimeters, measurement of the xylem flow and hydrological balance (Jensen *et al.*, 1990). Direct methods are more accurate, but due to difficulties in their application, indirect methods are more commonly used (Sánchez Martínez, 2001).

Several methods exist, with different complexity level, for the indirect determination of the evapotranspiration of crops (Doorenbos & Pruitt, 1976). The methods are based on: (i) air temperature and astronomic data (Thornthwaite, 1948; Blaney & Criddle, 1950); (ii) temperature and relative

humidity (Papadakis, 1965; Ivanov, 1954; Hargreaves, 1974); (iii) solar radiation (Turc, 1961; Jensen & Haise, 1963); (iv) mass and energy balance (Penman, 1948; Penman-Monteith (Monteith, 1965); (v) relation between the tank evaporation and the evapotranspiration (Kashyap & Panda, 2001). Other methods using acquisition and analysis of data from remote sensors have been developed to estimate the evapotranspiration of crops (Courault *et al.*, 2005; Gordillo Salinas *et al.*, 2014).

Even though all the mentioned methods are widely used, to understand the intervening factors and estimate the water demand of the crops, it is advisable to consider the continuous soil-plant-atmosphere. Any attempt to attribute the evapotranspiration process to only one factor can be useless or misleading (Sharma, 1985). In this sense the emergence of mathematical models to estimate the water demand means an advance in the understanding and quantification of the evapotranspiration in crops (Sellers *et al.*, 1986; Norero, 1987; Flerchinger & Pierson, 1991). In 1969, Norero proposed a new term: maximum evapotranspiration (ET_{max}) (Taylor & Ashcroft, 1973), to account for the maximum demand of water of a crop without limitations of any kind and with full supply of soil water. For the calculation of ET_{max} the energy balance in the crop has to be considered, with main phytometrics variables of the crops. The calculation has an academic value since

it can follow the evolution of the evapotranspiration with space resolution, even a particular soil layer within the canopy, and with a time resolution down to one hour or less. Practicality is another advantage of the use of ETmax, since it neither requires a reference crop, nor an evaporation tank or specific coefficients.

The central aim of this work is to show a mathematical model that allows estimation of the crop ETmax, given some phytometrics and meteorological characteristics.

MATERIALS AND METHODS

The mathematical model is based on two fundamental concepts: maximum evapotranspiration (ETmax) (Norero, 1969, cited by Taylor & Ashcroft, 1973); and the energy and radiation balance at the level of the crop, assuming that the hydric balance is closely connected with the energy balance (Hillel, 1980). The model was coded with "macros" of Visual Basic to be used in Microsoft® Excel.

Model description

The energy balance of the ten foliar layers constituting the crop is considered in detail. The simplified expression balances the net radiation (Rn) with the latent (ζE), sensitive (H) and edaphic (G) heats ($\text{MJ m}^{-2} \text{d}^{-1}$):

$$Rn = \zeta E - H - G = 0 \quad (1) \quad (\text{MJ m}^{-2} \text{d}^{-1})$$

At the same time, the net radiation is calculated from the radiation balance, which is due to the balance of direct (Rdn), diffuse (Rdfn) and long wavelength (RLn) radiation:

$$Rn = Rdn + Rdfn + RLn \quad (2) \quad (\text{MJ m}^{-2} \text{d}^{-1})$$

The model allows time steps down to a single minute, for which the sun position is calculated from the zenith (z) and azimuth (Az) angles. These angles depend on the site latitude (L), astronomic time (h) and solar declination (δ). Besides the sun position, also the intensity of the extra-atmospheric solar radiation (Ra) as a function of the average Earth-Sun distance, the solar constant (S) and the zenith angle (z), were calculated. And finally, the solar radiation reaching the crop (Rs), is estimated from Ra that includes the direct and diffuse components, according to the cloudiness, the cloud type, and the solar elevation angle (β) (Appendix A).

For the phytometric characterization the crop was arbitrarily divided in 10 foliar layers, with a time step down to minutes. This spatial and time resolution allows following the dynamics and anisotropy of the canopy. The direct radiation balance was calculated for each foliar layer, and according to the extinction coefficient estimated from the model proposed by Mann *et al.*, (1980) and developed by Bouzo (2004). Required data are: crop height (H), distance between rows (Lr), row azimuth (Azc), plant width (Lc), leaf area index (L), leaf insertion angle (α) and population density (σ). The diffuse radiation balance uses extinction coefficients assuming random oriented leaves (Oker-Blom & Kellomäki, 1982). The crop albedo (α_p) is calculated from the solar elevation angle (β) and its value for the different layers in the canopy is given by an allocation factor (r). This factor accounts for the obstruction to sunlight caused by each layer. The long wavelength balance uses the extinction coefficients from the model of Mann *et al.*, (1980), assuming vertical radiant fluxes. This balance considers the soil infrared radiation (RLS), the infrared

emission of each foliar layer (RLi) and the atmospheric radiation (RLA). The mathematical equation describing the long wavelength radiation for each layer follows the Stefan-Boltzman law.

The calculation of the latent heat flux (ζE) for each foliar layer and the soil surface, considers the water vapor conductivity coefficient (k_v) and the vapor pressure gradient between each level (e) and the external air (ea). The conductivity coefficient value was modified according the density (ρ), the air specific heat (cp), and the psychrometric constant (γ). In analogy to electrical circuits, the effect of the calculated series resistance ($\sum r_v$) for each level considered, is inversely proportional to the maximum evaporation estimation of the soil surface (E_s) as well as the leaves (E_i), up to a reference height above the crop:

$$\zeta E_i = k_{vi} \cdot (e_{fi} - ea) \cdot Li \quad (3)$$

$$\zeta E_s = K_{vs} \cdot (e_s - ea) \quad (4)$$

The sensible heat flux (H) was calculated as function of the conduction heat coefficient (k_c) and the thermal gradient between the considered level (T_{fi}) and the external air (T_a). The conduction coefficient was inverse proportional to the resistance sum ($\sum r_c$) and directly proportional to the density (ρ) and air specific heat (c_p) of the leaves (H_i) as well as the soil surface (H_s):

$$H_i = k_{ci} \cdot (T_{fi} - T_a) \quad (5)$$

$$H_s = k_{cs} \cdot (T_s - T_a) \quad (6)$$

In the calculation of the resistance involved in the heat and vapor dissipation, the wind acts as a regulator of the sensible and latent heat losses, respectively. For this

reason, the aerodynamics of the canopy and the soils surface were calculated from the wind speed above the crop (u). The movement quantity striking over and in the interior of the plant population, was calculated from the phytometric characteristics of the crop, this being considered as an energy dissipation entity of the movement quantity. The wind profile changes according atmospheric conditions of stability, instability or neutrality. The soil heat flux (G) was calculated in a simplified manner, assuming a dependence of the soil sensible heat (H_s). The higher the H_s , the smaller the G value will be. For this an allocation factor was calculated (τ), dependent of the wind speed (u) and the crop height (H):

$$G = \tau \cdot H_s \quad (7)$$

Finally, the balance results of the ten foliar layers that artificially dividing the canopy and the surface soil, formed a system of eleven equations with eleven unknowns. These unknowns are the temperatures of each level leaves and of the soil surface. From these temperature values, the layer of evaporated water can be determined. In this calculation the temperatures are the dependent variable of the vaporization latent heat (ζ) and of the vapor pressure at each level (e_i). The vapor pressures are assumed saturated at the supposed maximum evapotranspiration.

The variables for the model are space, time, variables proper of the crop and the meteorology (Fig. 1). The model simulates the intermediate variables in the different levels of the crop canopy: air temperature ($^{\circ}\text{C}$), wind speed (m s^{-1}), vapor pressure (kPa), latent and sensible heats ($\text{MJ m}^{-2} \text{d}^{-1}$), and net radiation ($\text{MJ m}^{-2} \text{d}^{-1}$). Finally, solving the energy and mass balances for each

time value gives the corresponding layer of maximum evapotranspiration (ETmax) (mm día⁻¹) (Fig. 1), by means of a daily integration of the calculated values of maximum evaporation and maximum transpiration (mm min⁻¹).

Model evaluation

For the comparison of the model with experimental data, the results from corn, sunflower, cotton and potato crops were used, as well as data from the literature. In this last case only well documented experiments were used, in order to have all the input data required by our model. The quality of the simulation was assessed by the Mean Square Error (RMSE), that evaluates the difference between the estimator (simulation value) and what is estimated (experimental value) data:

$$RMSE = \sqrt{\frac{\sum_{i=1}^N (\text{Experiment} - \text{Simulation})^2}{N}}$$

RESULTS AND DISCUSSION

Solar radiation regime

The diurnal solar radiation variation pattern is approximately sinusoidal over day (Shevenell, 1999). This result was verified by comparing the simulated results from the model and the experiments of Monteith & Unsworth (1990), in Rothamsted (52°N, 0°W). Very good agreement was found as seen from the low value of the calculated RMSE (Fig. 2). The observed curves correspond to three days with different lengths and irradiances, and visually show the good agreement between the simulation and the experiment, besides the calculated RMSE.

The radiation striking on the earth surface is affected mainly by two factors mod-

ifying the atmosphere transparency grade: the type and percentage of clouds present, and the angle of solar elevation. To validate the simulation, given by the model using experimental input data, three measured situations were used: totally clear sky, sky covered with altocumulus and with nimbostratus (Monteith & Unsworth, 1990) (Fig. 3). The obtained results showed the influence of the sky state and the solar elevation angle on the received global radiation (MJ m⁻² d⁻¹). The differences between the experimental data and the simulated results obtained with the model, under the same conditions were negligible, with a RMSE close to zero (Fig. 3).

The similar behaviour and the good approximation between the simulated results and the experimental data, show the accuracy of the model in the estimation of the solar radiation or global radiation affecting the crop (Figs. 2 and 3). The simulated cases included the presence of clouds in the condition of totally clouded sky. The abscissa is the solar elevation angle, showing an increase of the transmitted radiation with the increase of the solar elevation over the horizon. Besides, the arrows in the graph point out the intensity of the extra-atmospheric radiation (Angot values) only for 10°, 30° and 50° of solar elevation (or too solar altitude). These radiation values allow establishing the atmospheric transparency related to the transmitted radiation. For the case of a clear sky and with 50° of solar elevation, the atmospheric transparency was 76 %, while for altocumulus and nimbostratus it was 61 % and 14 %, respectively (Fig. 3).

Once the solar radiation strikes on the crop, a part of it is reflected by the albedo of the vegetation, which varies according the own characteristics of the crop, the en-

Fig. 1: Description of the model for the estimation of the maximum evapotranspiration in crops, showing the input variables and the model predictions (the intermediate dependent variables and the maximum evapotranspired layer of the crop).

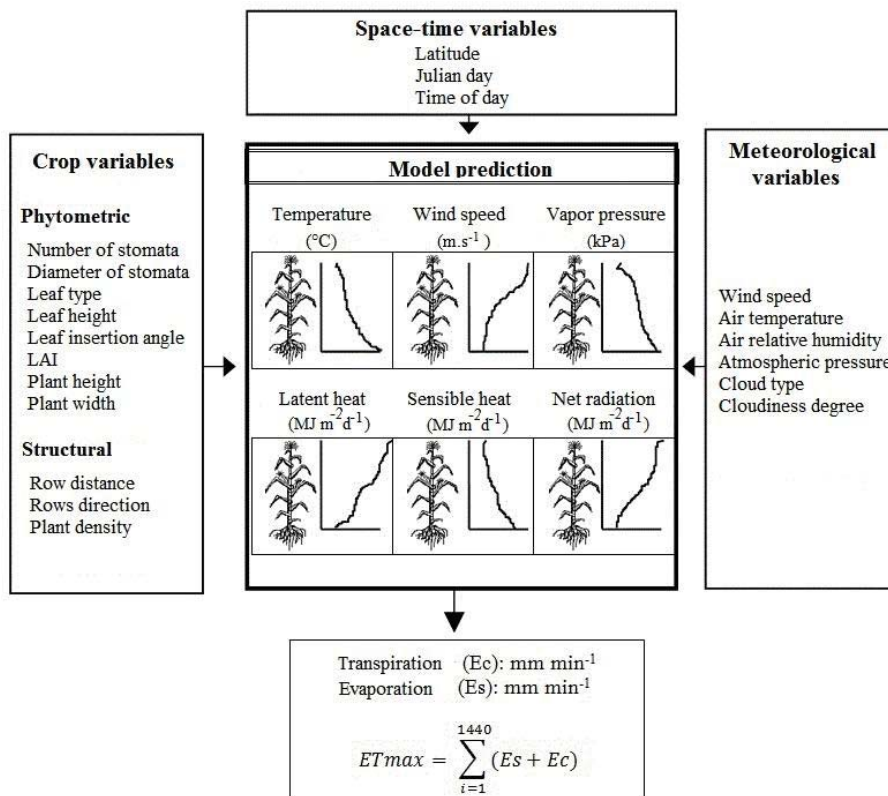


Fig. 2: Comparison of the simulated and measured (experimental) solar radiation (Monteith & Unsworth, 1990), for three clear days in Rothamsted (52°N, 0°W) with different photoperiods (h) and solar irradiance ($\text{MJ m}^{-2} \text{d}^{-1}$).

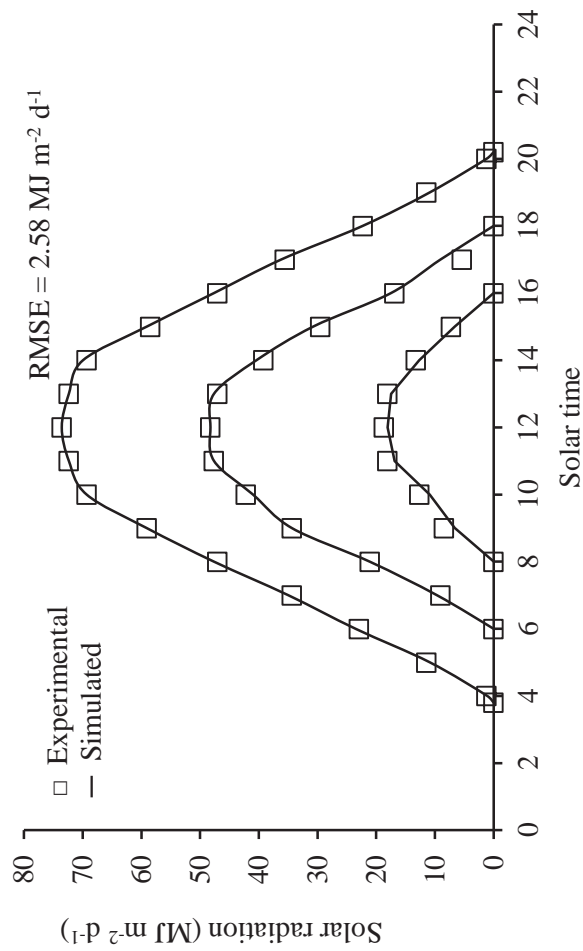
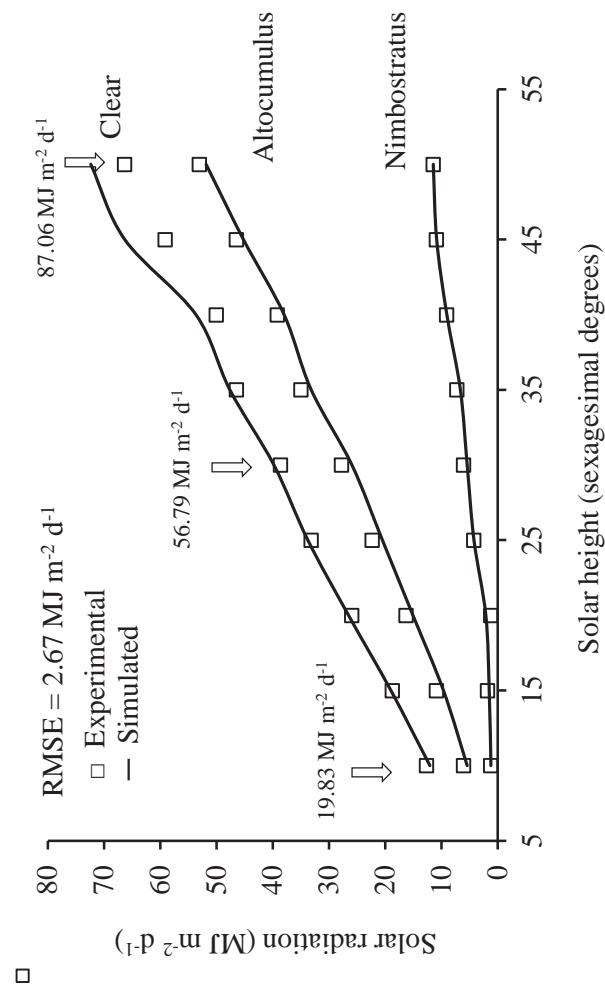


Fig. 3: Simulated and experimental results (Monteith & Unsworth; 1990) of the solar radiation given as the modifications of the solar height, in three different atmospheric situations during three days, with completely clear sky and with clouds of the kind altocumulus and nimbostratus.



vironment and the sun position. Due to the numerous intervening variables, it is difficult to get accurate values for each crop, having variations even between the morning and evening hours. The Fig. 4 shows the measurements from different authors for soybeans (André & Viswanadham, 1983), corn (Huber *et al.*, 1991, Sinoquet, 1989), cotton (Stanhill & Fuchs, 1968) and potato (Nkemdirim, 1973). The curve calculated with the model describes the albedo as a function of the solar altitude (Fig. 4).

Even though some dispersion between the simulated and experimental values is observed, the calculated RMSE is very low, showing the good agreement of the model. The albedo value is function of numerous factors participating of phenomenon of the solar light reflection on the crop, that is, the leaves positions, the cuticle characteristics, water condensation (i.e. dew), among others. However, besides the observed agreement here (Fig. 4), the predicted values by the model are within the range normally suggested in the literature (Monteith, 1965; Campbell, 1995).

The solar fraction reaching the crop and intercepted in the canopy, is a function of multiple factors proper of the crop, as well as astronomic and atmospheric. Huber *et al.*, (1991) performed measurements of the solar radiation intercepted by the canopy for a corn crop in Valdivia (Chile) (39° 48'S) at different times during the day over two days. The crop density was 55,000 pl ha⁻¹, sown with northeast-southeast orientation and a row separation of 0.70 m. Hourly measurements were done on January 12th and March 9th, with clear sky. For the first days, the plants had a height of 1.60 m and 2.15 of leaf area index of crop. Comparison of the percentage of solar radiation intercepted by the crop in both days, with the

model estimates, showed a linear correlation, with a variability of 75 %, explained by the model by the calculated determination coefficient (Fig. 5). The cloud of points in the graphic corresponded to the different situations determined by the height of the measurements of the interception in the crop and the time of the day.

In order to predict the transpiration as well as the photosynthesis, solar radiation intercepted by the crop must be known. In Fig. 5, the lower values shown correspond to the proportion of solar radiation that is finally transmitted to the soil. Exactly at these values the model gave the best prediction, considering a better correspondence with hypothetic function with slope 1 ($y = x$). In the interception higher values, the model showed a slight overestimation respect to experimental data (Fig. 5).

The distance between rows of plants is among the crop management practices influencing the capture of solar radiation, because it is one of the main factors affecting the extinction coefficient of crops (k). This was found in experiments (Mason *et al.*, 1982; Parvez *et al.*, 1989; Westgate *et al.*, 1997) where the rows distance was modified for crops of corn and soybean (0.35 m, 0.66 m y 1.00 m), with orientation north-south. In Fig. 6, the results of those measurements are shown together with extinction coefficients k , calculated from the measured radiation, given by $k = [-\ln(R_s/R_{s0})/L]$; where R_s is the radiation transmitted to the soil, R_{s0} is the radiation entering the canopy and L is the leaf area index. For the case of the corn and soybeans crops, the population densities were 74,000 pl ha⁻¹ and 228,000 pl ha⁻¹, respectively. These densities were maintained constant even when modifying the separation between rows.

With these experimental data also the

Fig. 4: Comparison of the albedo values simulated with the model, and experimental values from other authors, in different crops: soybean (*Glycine max L.*) (André & Viswanadham, 1983); corn (*Zea mays L.*) 1 (Huber et al., 1991) and 2 (Sinoquet, 1989); cotton (*Gossypium hirsutum L.*) (Stanhill & Fuchs, 1968) and potato (*Solanum tuberosum L.*) (Nkemdirim, 1973).

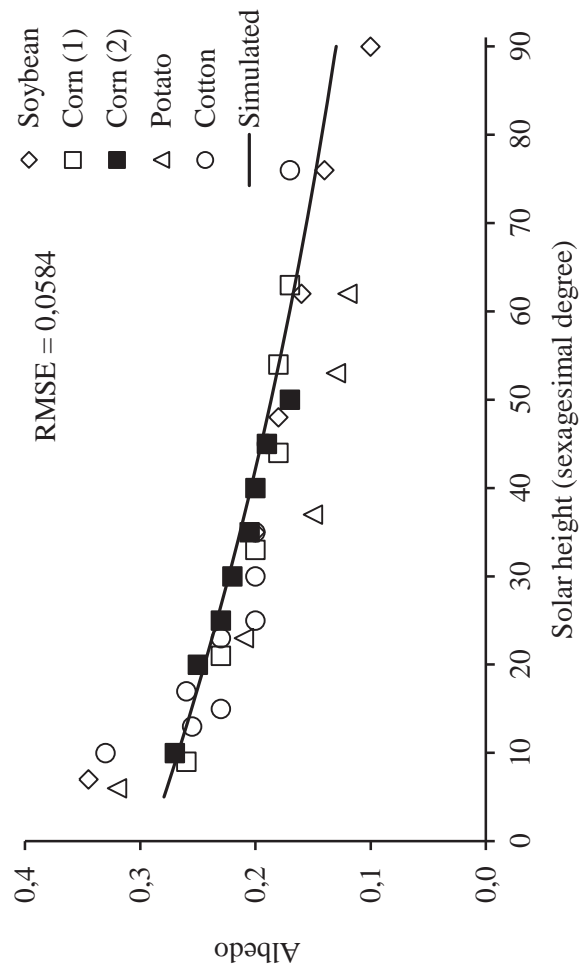
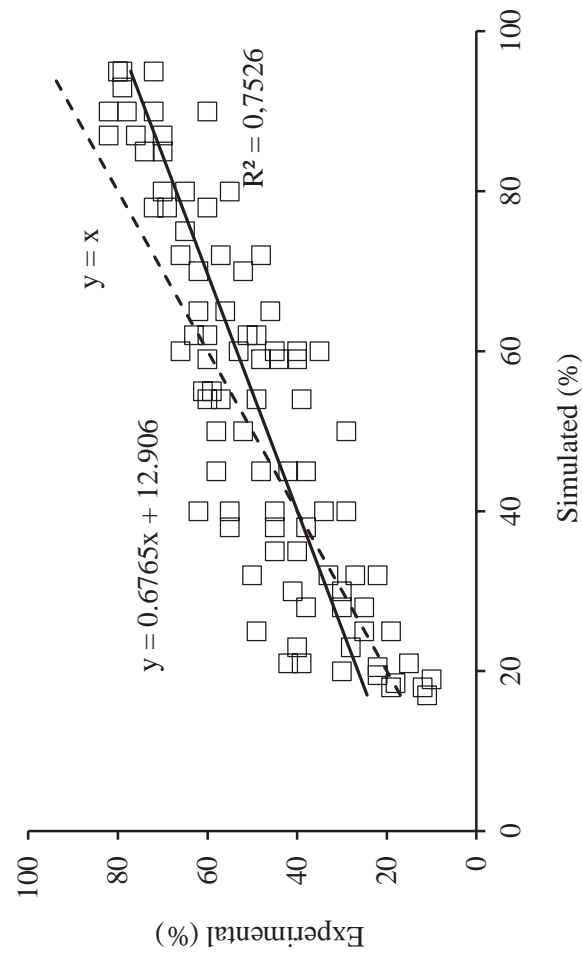


Fig. 5: Comparison of the simulated values and experimental data (Huber et al., 1991) of the percentage of intercepted radiation by a corn canopy (*Zea mays* L).



k values were simulated for corn (Fig. 6a) and soybeans (Fig. 6b). The agreement of the model was very good, with a better prediction for soybeans, as shown by the calculated RMSE low value.

Regime of wind speed

Wind is another important factor in the determination of the incident micrometeorological conditions on the crop. The aerodynamics characteristics on the crop are given in a great extent by the heat diffusion, the movement quantity, and the water vapor and carbon dioxide in the inner canopy environment. The prediction given by the model was compared with experimental data of a corn crop, where the wind speed profiles were measured above and inside the crop at different times of the day (Wright & Lemon, 1966). The crop had a density of 56,520 pl ha⁻¹ and a row separation of 0.75 m. In Fig. 7 the measured results and the model simulation are shown. The abscissa is the height (m) and the ordinate is the wind speed (m s⁻¹). A discontinuous vertical line points to the height (3 m) of the crop at the moment of the measurements. The continuous curves describe the wind profiles simulated at different times (11:00 am, 02:00 pm and 05:00 pm) (Fig. 7).

The observed differences between experimental and simulated values above the crop (> 3 m) were up to 0.2 m s⁻¹. However, once in the interior of the canopy (< 3 m) the model values showed a good agreement with the experimental values, with an observed value at most of 0.1 m s⁻¹. Towards the interior of the canopy, other friction forces operate, which are different from those at the upper part of the crop (Teh, 2006), like the plant height, density and leaf insertion angle. Though in general the model results slightly underestimated the

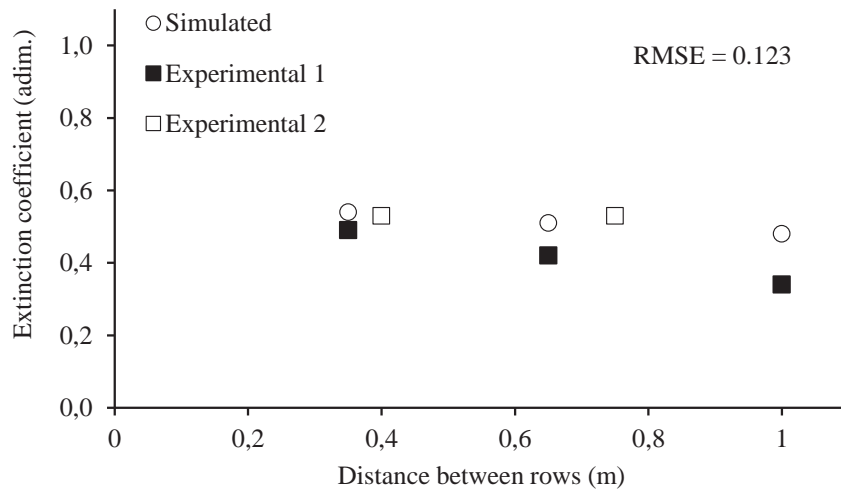
experimental values, the model followed the general trend of the experiment (Fig. 7).

Net radiation

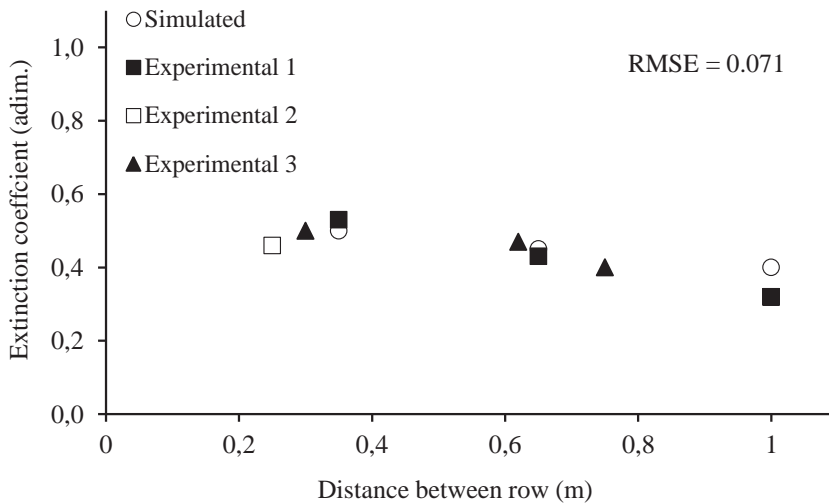
The net radiation in the phytosphere is fundamental for the description of the physical environment of the crops, and among other aspects, it represents the energy available for the crop growth, as well as the energy dissipated by the phenomena related to latent and sensible heat. Sufficiently documented experimental data of a soy crop was gathered to evaluate the results of the simulation of the net radiation (Baldochi *et al.*, 1981). The population density was 260,000 pl ha⁻¹ with row distance of 0.75 m, an average crop height of 1.45 m and a foliar area index of 4.1. The experimental conditions of the mentioned authors were reproduced using the model. The values of the measured solar radiation (Rs) and the experimental and simulated net solar radiation (Rn) are shown, as function of the solar hour for August 4th in the north hemisphere (41° 09' N) (Fig. 8).

The predictions from the model followed the trends in the experimental values, though some underestimate was observed at the beginning of the daytime (Fig. 8). The relation between the net and global radiation resulted in an average of 0.56 with an increase to the value of 0.68 in the noon solar time. These results are a good approximation to the experimental data for daytime of other authors (Graham & King, 1961; Tanner & Lemon, 1962). Since the radiation balance or net radiation can be expressed in a budget equation, composed of different terms that each represent a radiation transport or conversion process in crops and soil, the denomination as phytosphere coined by Norero (1977) is the most appropriate to consider both systems.

Fig. 6: Comparison of the global extinction coefficients simulated by the model, and the experimental values, in crops of corn (*Zea mays L.*) (a) and soybean (*Glycine max L.*) (b), with population densities of 74,000 pl ha⁻¹ and 228,000 pl ha⁻¹, respectively and with different distances between rows. In corn: Experiment 1 (Flénet et al., 1996), Experiment 2 (Westgate et al., 1997). In soybean: Experiment 1 (Mason et al., 1982, Parvez et al., 1989, Flénet et al., 1996).



(a)



(b)

Fig. 7: Experimental (Wright & Lemon, 1966) and simulated results of the wind speed ($m s^{-1}$) above ($> 3 m$) and below ($< 3 m$) a corn crop (*Zea mays L.*) in three different times of the day.

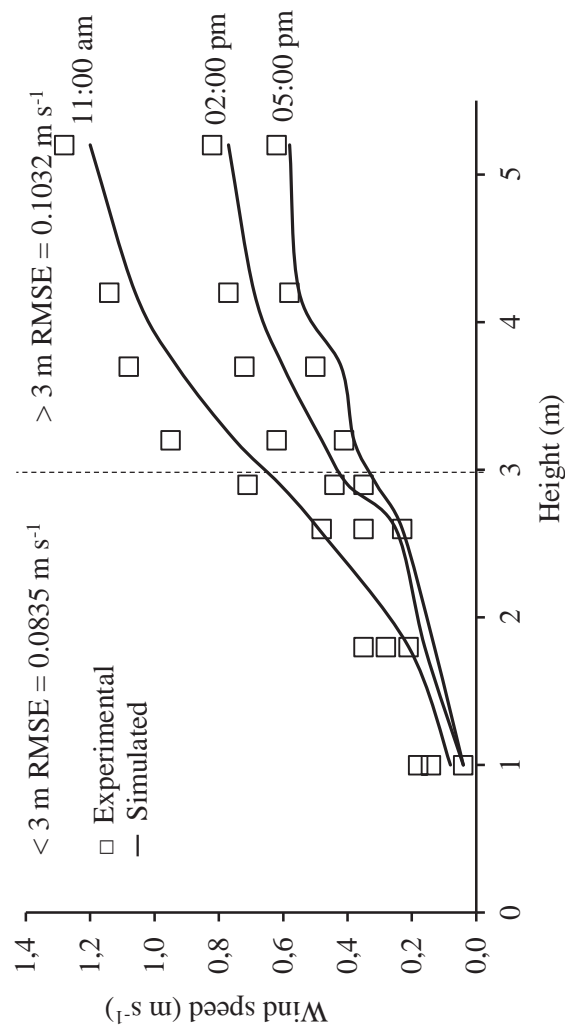
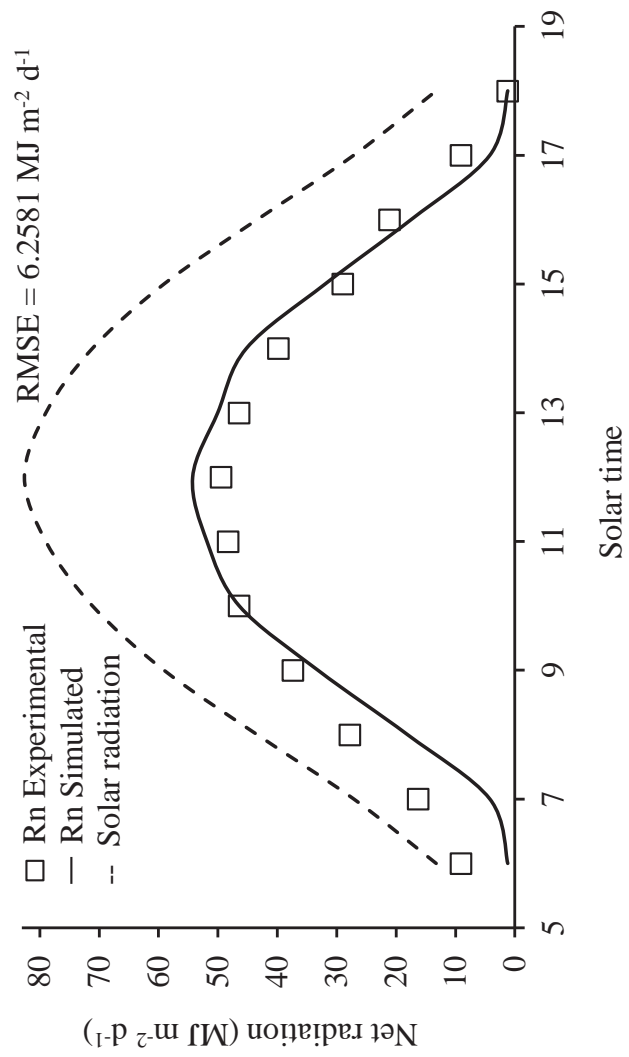


Fig. 8: Evolution of the measured solar radiation (R_s) and comparison of the simulated net radiation (R_n) and the measured experimental values (Baldochi et al., 1981) in a soybean crop (*Glycine max L.*) in Nebraska ($41^\circ 09' N$) on August 4th.



Though in the case studied above (Fig. 8) the net radiation of the phytosphere was evaluated, also the values of the radiation balances of the crop and the soil can be analyzed separately. For this purpose the experimental data of the cotton crop was used, with measurements of the net radiation ($\text{MJ m}^{-2} \text{d}^{-1}$) of the soil, the crop and the phytosphere. The crop under study had an average crop height of 0.49 m, a leaf area index of 1.7 and a population density of 180,000 pl ha^{-1} . The plant rows were oriented north-south with a separation of 1.0 m from each other (Ham *et al.*, 1991). The experimental data were plotted in a cartesian coordinates system with the solar hour in the abscissa (Fig. 9).

It is interesting noticing that the net radiation of the crop exceeded the value of the soil for the extreme hours of daytime, that is, first hours in the morning and last hours in the evening. While in the central hours, close to the solar noon, the net radiation on the soil slightly surmounted the values in the crop (Fig. 9). This behavior can be explained mainly by the fact that the crop was not completely developed, and then it is expected that an important proportion of soil is uncovered, resulting in more soil exposure during noon, emphasized by the orientation of the rows. The answers obtained by the model are in agreement with the cited experiment and with the results of Aubertin & Peters (1961).

Maximum evapotranspiration

Finally, it is fundamental to know how well the model of maximum evapotranspiration performed in comparison with the

most used procedure to estimate the potential evapotranspiration, that is the method of Penman-Monteith of the 1965.

First, the rate of water loss by transpiration and evaporation were simulated for the corn crop in Buin (Chile) ($33^{\circ} 33' \text{ S}$) on December 18th (Fig. 10). The calculation using the model of the maximum evapotranspired layer was performed with hourly frequency. The maximum evapotranspiration occurred at 15 h when the measured temperature in the fields reached the maximum value (29.9° C), and the lowest value for the air vapor pressure was registered (4.23 kPa) (meteorological data not shown). The average solar radiation at that time ($62.70 \text{ MJ m}^{-2} \text{ d}^{-1}$) was slightly lower than the maximum corresponding to the solar noon ($91.64 \text{ MJ m}^{-2} \text{ d}^{-1}$). However, the wind speed at 15 hs (2.8 m s^{-1}) was higher than at noon (1.4 m s^{-1}) explaining the higher demand of water at that hour (Fig. 10).

The integration of the areas under the curves allows obtaining the daily maximum evapotranspiration (ET_{max}) estimated by the model, resulting in 5.88 mm d^{-1} , while the reference evapotranspiration calculated by the Penman-Monteith method was 5.56 mm d^{-1} . Using a crop coefficient (kc) of 1.15 corresponding to a corn crop between the development stage 3 and 4 (Doorenbos & Pruitt, 1976; Doorenbos & Kassam, 1980). Another case for study was the sunflower crop (*Helianthus annuus* L.) in Curacaví (Chile) ($33^{\circ}25' \text{ S}$) on December 8th (Fig. 11). The maximum evapotranspiration estimated by the model was 7.54 mm d^{-1} while the reference evapotranspired calculated

Fig. 9: Changes in the measured solar radiation (Rs), and comparison of the net radiation (Rn) of soil, crop and phytosphere (Ham et al., 1991) and the simulated results for a cotton crop (*Gossypium hirsutum* L.) in Texas (33° 36' N) on August 3rd.

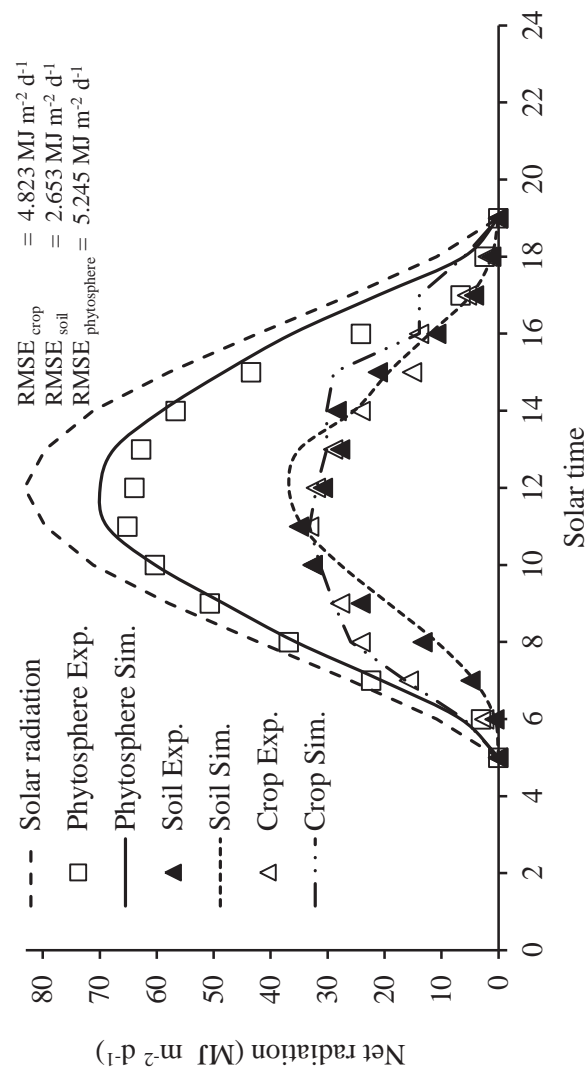


Fig. 10: Simulated maximum evapotranspiration of a corn crop (*Zea mays* L.) in Buin (Chile) ($33^{\circ} 33' S$) on December 18th. Measured data entered to the model: crop azimuth: 90° ; distance between rows: 0.70 m; population density: 60,000 pl ha⁻¹; average plant height: 1.35 m; maximum width: 0.60 m; IAF: 2.65; leaf insertion angles per layer (from top to bottom): 60° , 57° , 57° , 55° , 55° , 53° , 50° , 47° , 45° and 43° ; stoma diameter: 11 μm , stomata density (adaxial and abaxial leaf surfaces): 8,000 and 4,000 stomata cm⁻², respectively, leaf shape coefficient: 0.80 and leaf average width: 0.10 m.

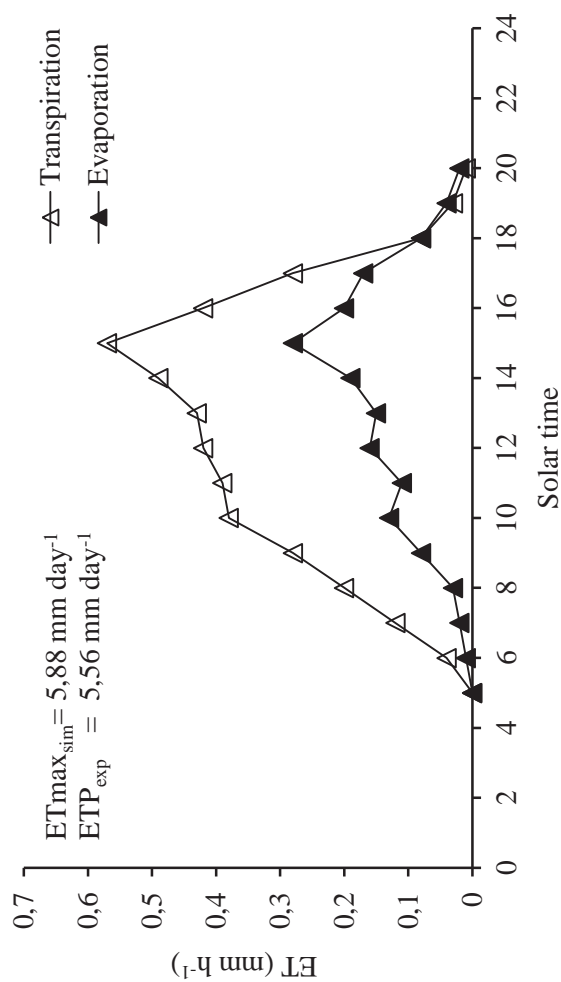


Fig. 11: Simulated maximum evapotranspiration for a sunflower crop (*Helianthus annuus* L.) in Curacavi (Chile) on December 8th. Measured data entered in the model: crop azimuth 90° (E-W), distance between rows: 0.70 m, population density of 56,000 pl ha⁻¹, average plant height: 0.95 m, maximum width: 0.36 m, leaf area index: 1.7, insertion leaf angle per layer (from top to bottom): 27°, 25°, 23°, 20°, 17°, 15°, 13°, 10°, 7°, 5°; stomata diameter: 15 μm, stomata density (adaxial and abaxial leaf surfaces): 8,500 y 15,600 stomata cm⁻², respectively, leaf shape index: 0.56, leaf average width: 0.22 m.

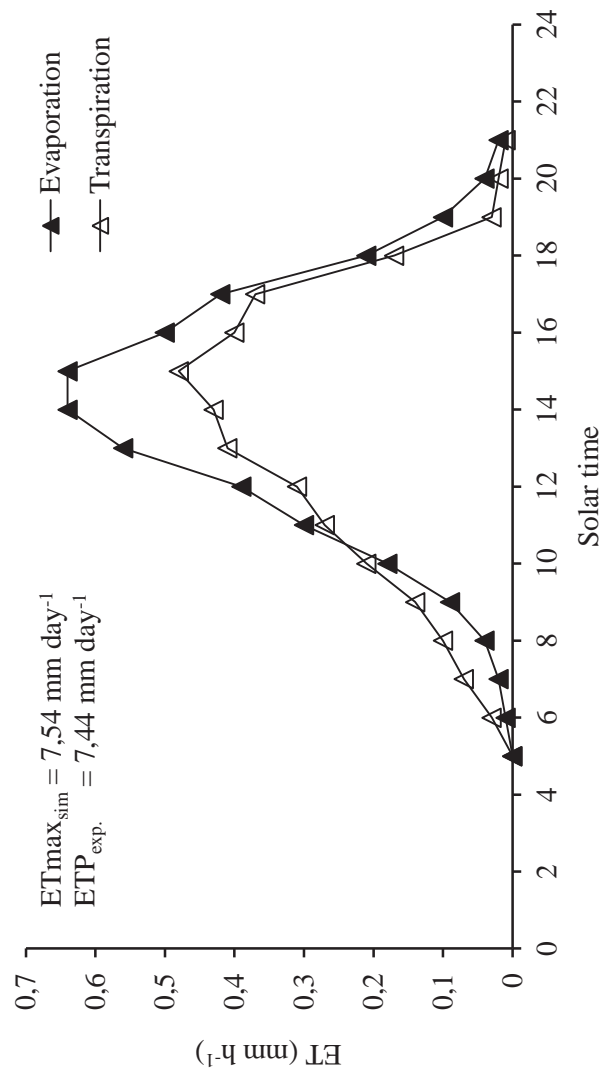
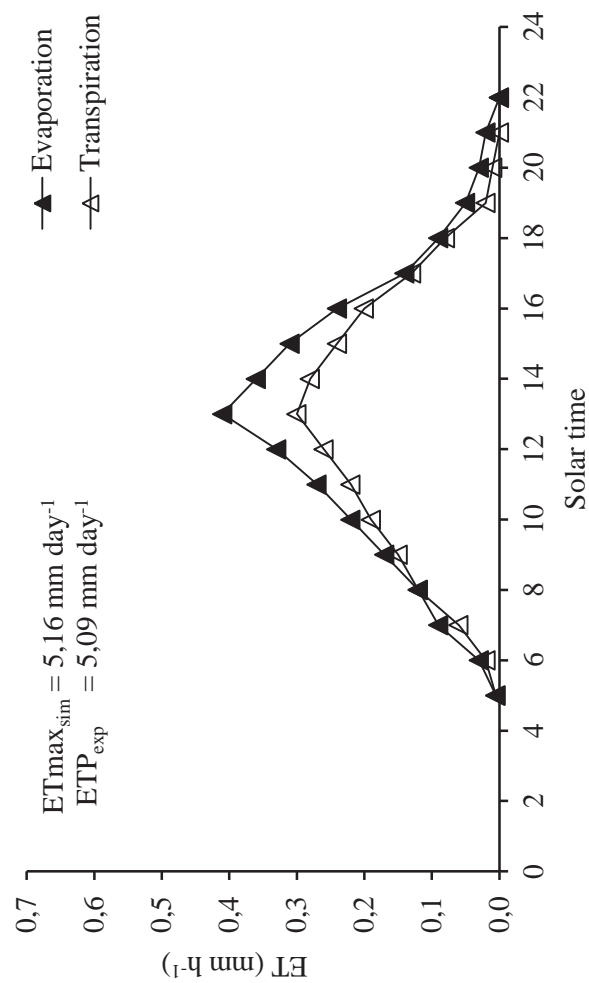


Fig. 12: Simulated maximum evapotranspiration for a potato crop (*Solanum tuberosum* L.) in Temuco (Chile) ($38^{\circ} 43' S$) on December 15th. Crop azimuth: 90° (E-W), distance between rows, 0.80 m, population density of $62,000 \text{ pl ha}^{-1}$, average plant height: 0.50 m, maximum width: 0.70 m, leaf area index: 1.50; leaf insertion angles per layer (top to bottom): $33^{\circ}, 30^{\circ}, 27^{\circ}, 25^{\circ}, 23^{\circ}, 20^{\circ}, 17^{\circ}, 15^{\circ}, 13^{\circ}$ and 10° ; stomata diameter $9.5 \mu\text{m}$, total leaf stomata density: $4,000 \text{ stomata cm}^{-2}$; leaf shape index 0.70; leaf average width 0.06 m.



by the Penman-Monteith method was 6.76 mm d⁻¹. Using a crop coefficient of 1.10 (Doorenbos & Kassam; 1980) corresponding to a sunflower crop in the middle of its development, a potential evapotranspiration (ETP) of 7.44 mm d⁻¹ was obtained.

In this case, and differently from the former case (Fig. 10), the soil evaporation surmounted the crop transpiration. This could be attributed to the scarce soil covering, as shown by the phytometric variables measured in the field and entered into the model. This situation increased at the time of the solar noon, when it is expected that the extinction produced by the crop decreased in a perceptible manner. The estimated values of the radiation extinction coefficient for the crop model were 0.54, 0.56 and 0.59 for 12, 13 and 14 h, respectively. While for 7 h the estimated extinction coefficient was 0.82, for a solar elevation angle of 24°. And last, the experimental data from a potato crop (*Solanum tuberosum* L.) in Temuco (Chile) (38° 43' S) on December 15th (Fig. 12) was used. The maximum evapotranspiration estimated by the model was 5.15 mm.day⁻¹. The evapotranspiration calculated by the Penman-Monteith method was 5.09 mm.day⁻¹, using a crop coefficient of 0.95 corresponding to a potato crop between the phenological stages 2 and 3 (Doorenbos & Kassam, 1980).

The maximum water loss of the crop occurred at 13 hs, in coincidence with the moment of the maximum measured temperature value (23.3° C), the minimum relative humidity (43 %) and the maximum wind speed (4,1 m s⁻¹) (meteorological data not shown). On the other hand, the solar radiation at this hour (88.63 MJ m⁻² d⁻¹) was not significantly different from the value

registered at noon (91.64 MJ m⁻² d⁻¹). The higher evaporation estimated here in relation to transpiration, similar to the sunflower, can be explained by the scarce foliar covering of the crop respect to the distance between rows.

CONCLUSIONS

The model shown in this work is based in the agro-physical analogy of the radiation and energy balance phenomenon in a crop. The model is especially appropriate for academic use, due to its ability to explain phenomena, which is given by the physical principles used and the resolution level used. The time interval of the model calculations, as well as the structural and functional aspects, allowed taking into account the anisotropy characteristic of the micrometeorology of the experimental crops used for comparison. The preliminary results shown here for the calculated maximum evapotranspiration using the model, give an acceptable behavior when compared with predictions obtained with the Penman-Montheit method. It remains to validate other situations, in order to incorporate different meteorology conditions and crop types.

APPENDIX A

List of equations

$$z = \arccos(\sin \phi \cdot \sin \delta + \cos \phi \cdot \cos \delta \cdot \cosh)$$

$$\delta = 0.006918 - 0.3999912 - \cos \theta - 0.070257 \cdot \sin \theta - 0.006758 - \cos 2\theta + 0.000907 \cdot \sin 2\theta - 0.002697 \cdot \cos 3\theta - 0.001480 - \sin 3\theta$$

$$\theta = 0.986 \cdot (J - 1) \cdot \frac{\pi}{180}$$

$$h = (12 - t_i) - 15 \cdot \frac{\pi}{180}$$

$$\beta = 90 - z \cdot \left(\frac{180}{\pi}\right)$$

$$A_z = \arcsin \left(\frac{\cos \delta \cdot \sin h}{\sin z} \right)$$

$$Ra = S \cdot \left(\frac{d_m}{d_r}\right)^2 \cos z$$

$$\left(\frac{d_m}{d_r}\right)^2 = 1.00011 + 0.033523 \cdot \cos(J') + 0.00128 \cdot \sin(J') + 0.000739 \cdot \cos(3J') + 0.000099 \sin(2J')$$

$$J' = \frac{2 \cdot \pi \cdot J}{365}$$

$$Rg = Ra \cdot (0.22766 \cdot \sin \beta + 0.6042) \cdot \left(1 - \frac{\eta}{100}\right)$$

$$Rd = Rg \cdot [0.81055991 \cdot (1.0095508 - \exp(-0.055407118 \cdot \beta))]$$

$$Rdf1 = Rg - Rd$$

$$Rdf2 = Ra \cdot \ln \left(\frac{\eta}{100}\right)$$

$$fn1 = 0.3403 \cdot \sin \beta + 0.3799$$

$$fn2 = 0.4318 \cdot \sin \beta + 0.3159$$

$$fn3 = 0.5302 \cdot \sin \beta + 0.2334$$

$$fn4 = 0.4393 \cdot \sin \beta + 0.1879$$

$$fn5 = 0.303 \cdot \sin \beta + 0.1697$$

$$fn6 = 0.1288 \cdot \sin \beta + 0.1598$$

$$fn7 = 0.1167 \cdot \sin \beta + 0.079$$

$$fn8 = 0.1393 \cdot \sin \beta + 0.027$$

$$fn9 = 0.0528 \cdot \sin \beta + 0.0203$$

$$H_{sr} = 12 - \left[\frac{h_{up} \cdot \left(\frac{180}{\pi}\right)}{15} \right]$$

$$h_{up} = \arccos(-\tan \phi \cdot \tan \delta)$$

$$H_{ss} = 24 - H_{sr}$$

$$N_d = 12 \cdot \left[1 + \left(\frac{2}{\pi}\right) \cdot \arccos \sin \left(\frac{\alpha}{\beta}\right) \right]$$

$$a = \sin \phi \cdot \sin \delta$$

$$b = \cos \phi \cdot \cos \delta$$

$$\alpha_s = -0.0392 \ln \beta + 0.3033$$

$$\alpha_p = 0.297327 \cdot \exp(-0.010679 \cdot \beta)$$

$$R_{df(i)} = R_{df} \cdot (1 - \alpha_{pi}) \cdot (1 - V_{sky}) \cdot [0.25 \cdot \exp(-1 - 1.93 \cdot L'_i) + 0.5 \cdot \exp(-0.707 \cdot L'_i) + 0.25 \cdot \exp(-0.518 \cdot L'_i)]$$

$$V_{sky} = \frac{\sqrt{[(L_r - L_c)^2 + H^2]}}{L_r} - H$$

$$L' = L \cdot \frac{L_r}{L_c}$$

$$RL = \varepsilon \cdot \sigma \cdot T^4$$

$$\varepsilon_a = 0.552 \cdot e_a^{0.1428}$$

$$RL_A = RL_{AD} + RL_{AN} \cdot \left(\frac{\eta}{100}\right)$$

$$T_\eta = T - 0.0065 \cdot Z_i$$

$$\varepsilon_\eta = 6.11 \cdot \exp \left[\frac{17.27 \cdot T_\eta}{237.3 + T_\eta} \right]$$

$$RN_{d1} = \left[Rd(1 - \alpha_{p1}) + Rd_{10} \cdot \alpha_s \cdot \exp(-L_i \cdot \sum_{i=1}^9 ki) \right] - \left[Rd_{10} \cdot \alpha_s \cdot \exp(-L_i \cdot \sum_{i=1}^{10} ki) + Rd \cdot (1 - \alpha_{p1}) \cdot \exp(-L_i \cdot k1) \right]$$

$$RN_{dsoil} = Rd_{10} \cdot (1 - \alpha_s)$$

$$\begin{aligned}
 RNL_1 &= \left[RL_{soil} \cdot \varepsilon_f \cdot \exp(-L' \cdot \sum_{i=10}^2 k_{Li}) + RL_A \cdot \varepsilon_f - RL_1 \right] \cdot (1 - \exp(-L' \cdot k_{L1}) \cdot r_L \\
 u_z &= \frac{u^*}{k} \ln \left(\frac{z-d}{z_0} \right) \\
 d &= 0.63 \cdot Hc \\
 z_0 &= 0.13 \cdot Hc \\
 u &= u_n \cdot \exp[-n \cdot (Hc - z)] \\
 n &= \sqrt[3]{\frac{D_f \cdot C_d}{4 \cdot l_{(h)}}} \\
 C_d &= 0.037 \cdot (1 + \alpha^n)^{2.708014} \cdot u^{-\left(\frac{0.3965}{\alpha \cdot 2.96582 + 1}\right)} \\
 l_{(h)} &= 12.3614 \cdot \left(\frac{z}{Hc}\right)^2 + 0.1562 \cdot \left(\frac{z}{Hc}\right) \\
 H_i &= 2 \cdot k_{Ci} \cdot (T_{fi} - T) \\
 k_{Ci} &= \frac{0.0004}{r_{Ci} + r_{fi} + r} \\
 r_{Ci} &= 0.005 \cdot \sqrt{\frac{af - wf}{u_{zi}}} \\
 r_{fi} &= 0.0009 \cdot u_H \cdot [1 \cdot \exp(-\gamma)] \cdot \left[\frac{\ln\left(\frac{7700}{Hc} - 5.92\right)}{u_{10}} \right]^2 \cdot \ln \left[\frac{(\exp \gamma) - 1}{\left[\exp\left(\gamma \cdot \frac{z_i}{Hc}\right) - 1\right]} \right] \\
 r &= \frac{0.0009}{u_{10}} \cdot \ln \left(\frac{7700}{Hc} - 5.92 \right) \cdot \ln \left(\frac{4400}{Hc} - 3.35 \right) \\
 \gamma &= (1.6 - 0.013 \cdot \alpha) \cdot L \\
 H_s &= k_{Cs} \cdot (T_s - T) \\
 k_{Cs} &= \frac{0.0003}{r_{Cs} + r_0 + r} \\
 r_{Cs} &= 0.00008 \cdot \frac{Hc}{u_{10}} \cdot \exp(0.9 \cdot \gamma) \\
 r_0 &= 0.0009 \cdot u_H \cdot [1 - \exp(-\gamma)] \cdot \left[\frac{\ln\left(\frac{7700}{Hc} - 5.92\right)}{u_{10}} \right]^2 \cdot \ln \left[\frac{(\exp \gamma) - 1}{\exp(0.1 \cdot \gamma) - 1} \right] \\
 E_i &= \xi \cdot k_{Vi} \cdot (e_{fi} - e_a) \cdot Li \\
 k_{Vi} &= \frac{7.5 \cdot 10^{-7}}{r_{Vi} + r_{fi} + r} \\
 r_{Vi(d)} &= \frac{0.002 + 3 \cdot p_i}{0.0015 + 2.25 p_i + 90 p_i^2 \cdot (n_1 + n_2)} + 0.004 \cdot \sqrt{\frac{af \cdot wf}{u_{zi}}} \\
 r_{Vi(n)} &= 1.33 + 0.004 \cdot \sqrt{\frac{af \cdot wf}{u_{zi}}} \\
 p_i &= p^* \text{ if } Rg \geq 0.2 \text{ cal cm}^{-2} \text{ min}^{-1} \\
 p_i &= 0.023 \cdot p^* \cdot \exp(18.8 \cdot Rg) \text{ if } Rg < 0.2 \text{ cal cm}^{-2} \text{ min}^{-1} \\
 p_i &= 0 \text{ if } Rg = 0 \\
 e_{fi} &= 6.11 \cdot \exp\left(\frac{17.27 T_{fi}}{237 + T_{fi}}\right) \\
 \xi &= 597.3 - 0.56 \cdot T \\
 E_s &= \xi \cdot k_{Vs} \cdot (e_s - e_a) \\
 k_{Vs} &= \frac{7.5 \cdot 10^{-7}}{r_{Vs} + r_0 + r} \\
 r_{Vs} &= 0.000065 \cdot \frac{Hc}{u_{10}} \cdot \exp(0.9 \gamma) \\
 \tau &= \frac{5.8 \cdot \ln(12900 \cdot \frac{u_{10}}{\sqrt{Hc}})}{u_{10} \cdot \sqrt{Hc}} \\
 RN_s &= (1 + \tau) \cdot Hs + Es
 \end{aligned}$$

APPENDIX B

List of Symbols

- a_f , leaf shape coefficient
 A_z , solar azimuth angle
 A_{rc} , row azimuth
 C_d , foliar drag coefficient
 C_p , air specific heat
 d , zero displacement plane
 D_f , leaf area density
 d_m , average Earth-Sun distance
 d_r , real Earth-Sun distance
 e , vapor pressure
 e_a , vapor pressure air.
 f_n , cloud factor. (1. irregular low clouds; 2. cirrus cloud; 3. high cumulus cloud; 4. cirrus stratus cloud, 5. stratus cumulus cloud, 6. high dense stratus; 7. dense layers of stratus and stratuscumulus clouds; 8. nimbu stratus clouds, 9. mist.
 G , edaphic heat
 H , sensitive heat
 h , solar hour angle.
 H_c , crop height
 H_i , Sensible heat flux in foliar level (i).
 H_{sr} , sunrise time
 H_{ss} , sunset time
 h_{up} , intermediate variable
 J , julian day.
 k , Von Karman's constant (=0.41)
 k_{ci} , coefficient of heat conductivity of the layer i
 K_{CS} , heat conductivity of the soil surface
 K_v , vapor conductivity coefficient
 $l_{(h)}$, mixing length.
 L , leaf area index
 L_c , plant width
 L_r , distance between rows
 n , adimensional variable
 p^* , maximum stomatal aberture.
 p_i , stomatic aberture.
 r , allocation factor
 r , atmospheric resistance layer on the crop to heat sensible and latent exchange
 R_a , extra-atmospheric solar radiation (angot)
 r_{ci} , leaf resistance to heat flow at level i
 R_d , direct solar radiation.
 $R_{d(i)}$, diffuse solar descendent in the canopy
 R_{dfl} , difuse solar radiation whitout clouds
 R_{d12} difuse solar radiation with clouds
 R_{dfln} , net difuse radiation
 R_{dn} , net direct radiation
 r_{fi} , Interfoliar resistance at level i.
 R_g , global radiation
 RL , long wavelength radiation.
 RL_{AD} , longwave radiation with clear sky
 RL_{AN} , longwave radiation with cloudy sky
 RL_i , infrared emission of foliar layer 'i'.
 RL_n , Net long wavelength radiation
 RL_s , soil infrared radiation
 Rn , net radiation
 RN_{d1} , net radiation directly to the leaf level 1
 RNd_{soil} , net radiation directly to the soil
 RNI_1 , net radiation wavelenght to the leaf level 1
 T , air temperature.

T_f . foliar level (i) temperature.
 t_i . time of day.
 T_s . soil temperature
 T_{η} temperature cloudbase.
 $u_{(h)}$. wind speed on the crop
 u^* . friction wind speed.
 u_{10} . speed wind at 10 m
 uz . profile of speed wind
 V_{sky} . ground 'view' factor.
 w_f . average width of the leaf
 z . height
 Z . solar zenith angle
 z_0 . roughness length
 Z_d . average cloud height.
 A . leaf insertion angle
 α' . average angle of insertion foliar
 α'' leaf insercion angle in radians
 α_p . crop albede
 α_s . soil albede
 β solar elevation angle
 γ extinction coefficient of the wind in the canopy
 δ . solar declinatio in radians.
 ϵ_a atmosphere emissivity
 ϵ_{η} cloud emittance.
 ζE . latent heat
 η percentage of cloudy sky.
 θ day of the year in radians.
 ρ . air density.
 σ . plant population density
 ϕ . latitude in radians
 γ . psychrometric constant.

LITERATURA CITED

- 1.- ALLEN, R.; PEREIRA, L.; RAES, D. & SMITH, M. 1998. Crop evapotranspiration. Guidelines for computing crop water requirements. FAO Irrigation and Drainage Paper, 56. Rome. 300 p.
- 2.- ANDRÉ, R.G.B. & VISWANADHAM, Y. 1983. Radiation balance of soybeans grown in Brazil. Agr. Meteor. 30:157-173.
- 3.- AUBERTIN, G.M. & PETERS, D.B. 1961. Net radiation determinations in a corn field. Agron. J. 53:269-272.
- 4.- BALDOCHI, D.D.; VERMA, S.B. & ROSENBERG, N.J. 1981. Mass and energy exchanges of a soybeans canopy under environmental regimes. Agron. J. 73:706-710.
- 5.- BLANEY, H.F. & CRIDDLE, W.D. 1950. Determining water requirements in irrigated areas from climatological and irrigation data. U.S. Dept. Agr. Soil. Conserv. Serv. SCS-TP-96. 44 p.
- 6.- BOUZO, C.A. 2004. Régimen de radiación diurno en cultivos en hileras. In: Simulación de Cultivos Anuales. Formulacións básicas del desenvolvimiento normal, Pilatti, M.A., Norero, A.L. (eds.). Ediciones UNL, Santa Fe, Argentina 64-77.
- 7.- CAMPBELL, G.S. 1995. Introducción a la biofísica ambiental. EUB Ed. Barcelona. 188 pp.
- 8.- COURAULT, D.; SEGUIN, B. & OLIOSO, A. 2005. Review on estimation of evapotranspiration from remote sensing data:

- From empirical to numerical modeling approaches. *Irrigation and Drainage Systems*. 19(3-4):223-249.
- 9.- **DOORENBOS, J. & PRUITT, W.O.** 1976. Las necesidades de agua de los cultivos. FAO. Roma 192 p.
- 10.- **DOORENBOS, J. & KASSAM, A.H.** 1980. Efectos del agua sobre el rendimiento de los cultivos. *Estudios FAO Riego y Drenaje* 33. Roma. 212 p.
- 11.- **FLÉNET, F., KINIRY, J.R., BOARD, J.E., WESTGATE M.E. REICOSKY, D.C.** 1996. Row Spacing Effects on Light Extinction Coefficients of Corn, Sorghum, Soybean, and Sunflower. *Agron. J.* 88(2):185-190.
- 12.- **FLERCHINGER, G.N. & PIERSON, F.B.** 1991. Modeling plant canopy effects on variability of soil temperature and water. *Agric. For. Meteorol.* 56:227-246.
- 13.- **GORDILLO SALINAS, V.M.; MAGDALENO, H.F.; TIJERINA CHÁVEZ, L. & ARTEAGA RAMÍREZ, R.** 2014. Estimación de la evapotranspiración utilizando un balance de energía e imágenes satelitales. *Revista Mexicana de Ciencias Agrícolas* 5(1):143-155.
- 14.- **GRAHAM, W.G. & KING, K.M.** 1961. Fraction of net radiation utilized in evapotranspiration from a corn crop. *Soil Sci. Soc. Am. Proc.* 25:158-160.
- 15.- **HAM, J.M.; HELLMAN, J.L. & LASCANO, R.J.** 1991. Soil and canopy energy balances of a row crop at partial cover. *Agron. J.* 83:744-753.
- 16.- **HARGREAVES, G.H.** 1974. Estimation of potential and crop evapotranspiration. *Transactions of the ASAE* 17(4):701-704.
- 17.- **HILLEL, D.** 1980. Applications of soil physics. Academic Press. 385 p.
- 18.- **HUBER, A.W.; BRAHM, R. & BRÜMMER, R.** 1991. Variación temporal del albedo en un cultivo de maíz (*Zea mays* L.) en el sur de Chile (Valdivia, X Región). *AgroSur*. 19(2):117-123.
- 19.- **IVANOV, N.N.** 1954. About potential evapotranspiration estimation. *Izvestiia Vsesoiuznogo Geograficheskogo Obschetva*. 86:189-195. (In Russian).
- 20.- **JENSEN, M.E. & HAISE H.R.** 1963. Estimating evapotranspiration from solar radiation. *Journal of Irrigation and Drainage Engineering*. American Society of Civil Engineers. 89:15-41.
- 21.- **JENSEN, M.E.; BURMAN, R.D. & ALLEN, R.G.** 1990. Evapotranspiration and Irrigation Water Requirements. American Society of Civil Engineers. *Manual of Practice* 70. New York. 360 p.
- 22.- **KASHYAP, P.S. & PANDA, R.K.** 2001. Evaluation of evapotranspiration estimation methods and development of crop-coefficients for potato crop in a sub-humid region. *Agricultural Water Management*. 50(1):9-25.
- 23.- **LU, J.; SUN, G.; MCNULTY, S.G. & AMATYA, D.M.** 2005. A comparison of six potential evapotranspiration methods for regional use in the southeastern United States. *Journal of the American Water Resources Association* 41(3):621-633.
- 24.- **MANN, J.E.; CURRY, G.L.; DEMICHELE, D.W. & BAKER, D.N.** 1980. Light penetration in a row-crop with random plant spacing. *Agron. J.* 72:131-142.
- 25.- **MASON, W.K.; ROWSE, H.R.; BENNIE, A.T.P.; KASPAR, T.C. & TAYLOR, H.M.** 1982. Responses of soybeans to two row spacings and two soil water levels. II. Water use, root growth and plant water status. *Field Crops Research*. 5:15-29.
- 26.- **MONTEITH, J.L.** 1965. Evaporation and environment. The estate and movement of water in living organisms. 19th Symp. Soc. Exp. Biol. U.K. 19:205-234.

- 27.- **MONTEITH, J.L. & UNSWORTH, M.H.** 1990. Principles of environmental physics. 2nd. edit. Edward Arnold. 291 p.
- 28.- **NKEMDIRIM, L.C.** 1973. Radiative flux relations over crops. *Agr. Meteor.* 11:229-242.
- 29.- **NORERO, A.L.** 1977. La fitosfera: el ambiente físico de las plantas. *Ciencia e Investigación Agraria* 4(4):263-272.
- 30.- **NORERO, A.L.** 1987. Requerimiento de agua de los cultivos. Modelo 1. Proyecto 061/87. DIUC. Facultad de Agronomía. Pontificia Universidad Católica de Chile. 175 pp.
- 31.- **OKER-BLOM, P. & KELLOMÄKI, S.** 1982. Effect of angular distribution of foliage on light absorption and photosynthesis in the plant canopy: theoretical computations. *Agr. Meteor.* 26:105-116.
- 32.- **PAPADAKIS, J.** 1965. Potential evapotranspiration. *Soil Sci.* 100(1), 76 p.
- 33.- **PARVEZ, A.Q.; GARDNER, F.P. & BOOTE, K.J.** 1989. Determinate and indeterminate type soybean cultivar responses to pattern, density and planting date. *Crop Sci.* 29:150-157.
- 34.- **PENMAN, H.L.** 1948. Natural evaporation from open water, bare soil and grass. *Proc. Roy. Soc. London.* 193:120-146.
- 35.- **SÁNCHEZ MARTÍNEZ, M.I.** 2001. Métodos de estimación de evapotranspiración utilizados en Chile. *Rev. Geogr. Norte Grande.* 28:3-10.
- 36.- **SELLERS, P.J.; MINTZ, Y.I.; SUD, Y.C. & DALCHER, A.** 1986. A simple biosphere model for use within general circulation models. *J. Atmos. Sci.* 43:505-531.
- 37.- **SHARMA, M.L.** 1985. Estimating evapotranspiration. *Advance in Irrigation.* 3:213-281.
- 38.- **SHEVENELL, L.** 1999. Regional potential evapotranspiration in arid climates based on temperature, topography and calculated solar radiation. *Hydrological Processes.* 13(4):577-596.
- 39.- **SINOQUET, H.** 1989. Modésitaion de l'interception des rayonnments solaires dans une cultuture en rangs. I. Aspects théoriques. *Agronomie.* 9:125-135.
- 40.- **STANHILL, G. & FUCHS, M.** 1968. The climate of the cotton crop: physical characteristics and microclimate relationships. *Agr. Meteor.* 5:183-202.
- 41.- **TANNER, C.B. & LEMON E.R.** 1962. Radiant energy utilized in evapotranspiration. *Agron. J.* 54:207-212.
- 42.- **TAYLOR, S. & ASHCROFT, G.** 1973. Physical edaphology. The physics of irrigated and nonirrigated soils. Wilt Freeman and Company. San Francisco. 533 p.
- 43.- **TEH, C.** 2006. Introduction to mathematical modeling of crop growth. How the equations are derived and assembled into a computer model. BrownWalker Press. Florida. EUA. 256 p.
- 44.- **THORNTHWAITTE, C. W.** 1948. An Approach toward a Rational Classification of Climate. *Geographical Review.* 38(1):55-94.
- 45.- **TURC, L.** 1961. Evaluation des besoins en eau d'irrigation, évapotranspiration potentielle, formulation simplifié et mise à jour. *Ann. Agron.* 12:13-49.
- 46.- **WESTGATE, M.E.; FORCELLA, F. REICOSKY, D.C. & SOMSEN, J.** 1997. Rapid canopy closure for maize production in the northern US corn belt: Radiation-use efficiency and grain yield. *Field Crops Res.* 49(2-3):249-258.
- 47.- **WRIGHT, J.L. & LEMON, E.R.** 1966. Photosynthesis under field conditions. VIII. Analysis of windspeed fluctuation data to evaluate turbulent Exchange within a corn crop. *Agron. J.* 58:255-261.